Quantum State-Resolved Collision Relaxation of Highly Vibrationally Excited SO_2†

Min Zhang

Department of Chemistry, University of Pennsylvania, Philadelphia, Pennsylvania 19104-6323

Hai-Lung Dai*

Department of Chemistry, Temple University, Philadelphia, Pennsylvania 19122

Received: July 2, 2007; In Final Form: July 30, 2007

Collision depopulation cross sections of 13 single, highly vibrationally excited levels with 45 000 cm^{-1} energy in the electronic ground state of SO_2 in collision with CO in a supersonic jet have been measured. The measurements for these single highly excited quantum states are conducted through pressure dependence of the decay of the fluorescence quantum beat resulted from their coupling with the rovibronic levels in the optically allowed transitions to the (140), (210), and (132) $\tilde{C}^1B_2$ levels. The relaxation cross sections of these highly excited states, each with well-defined energy and symmetry, range from 27 to 187 $Å^2$ with an average of 71 $Å^2$. This average cross section is much larger than the hard sphere cross section of 48 $Å^2$. The relaxation cross section is also found to be larger for the quantum states with a larger matrix element in coupling with the "bright" electronically excited level. Both observations suggest a substantial contribution from long range interactions in collision relaxation of highly excited molecules.

I. Introduction

Relaxation of highly vibrationally excited molecules[1,2] plays a significant role in important chemical phenomena such as unimolecular reactions and photochemistry.[2−5] In these processes, the reaction of an excited molecule through a specific channel competes with intramolecular vibrational redistribution[6] and collision-induced intermolecular vibrational energy transfer.[1] Both processes reduce the energy available for the specific reaction to occur. In studies of intermolecular, collision-induced energy transfer, fundamental understanding and theoretical descriptions have been established for molecules excited at low, primarily the fundamental, vibrational levels.[7−9] Recent studies on collision energy transfer have focused on molecules excited with energies sufficiently high for reactions to occur as new experimental approaches[10,11] were developed for characterizing highly vibrationally excited molecules.[10,12]

To characterize collision energy transfer from highly excited molecules, ideally the measurements should be conducted with energy or state specificity for the excited molecules. But because of difficulties in preparation and detection, almost all studies have been done with a broad energy distribution among the excited molecules,[10,12,13] far from the single-state specificity condition.

Several laser-based experimental techniques, which include stimulated emission pumping[14] and single-photon overtone excitation,[15] have the potential for preparing single highly vibrationally excited state (HVES) in energy regions where the level density is sufficiently low in consideration of laser resolution. The kinetic quantum beat spectroscopy[16] is one approach that can facilitate HVES excitation with single-state specificity even in energy regions with high densities. This approach is feasible for molecules that display vibronic coupling between a fluorescing electronic state and its nearby ground electronic state high-vibrational levels. Quantum beat (QB)[17] is a phenomenon in which a periodic oscillation in time occurs in the intensity of the fluorescence induced by coherent excitation of a small number of molecular eigenstates. Fluorescence QB has been observed for quite a few molecules such as SO_2,[18] formaldehyde,[19] acetylene,[20] pyrazine,[21] biacetyl,[22,23] and even the HCCS radical.[24]

The simplest case in QB arises from coherent excitation of only two eigenstates that are related to a coupling between two zero-order levels: one optically "bright" level that can be accessed through optical excitation and provide the oscillator strength for fluorescence and the other the optically "dark" level. Coherent excitation of the two eigenstates[17] results in the initial preparation of the optically bright level wavefunction followed by an oscillation of the amplitudes of the bright and dark level wavefunctions in time. This evolution of wavefunction in time is mimicked by the oscillation of the fluorescence intensity, which is proportional to the bright level wavefunction amplitude squared. The dark level wavefunction is also excited, and its amplitude oscillates as the balance of the bright level wavefunction. Consequently, coherent excitation of the pair of molecular eigenstates provides a "window" through which the dark level wavefunction can be accessed and excited.[16,25,26]

Previously, QB spectroscopy has been mostly used for probing singlet−triplet coupling.[22,27] Zeeman anticrossing spectroscopy has been developed to characterize intramolecular coupling through controlling the coupling strength using an external magnetic field.[19,20,27] In the large molecule limit, QB spectroscopy has been used to probe intramolecular relaxation as coherent excitation can be used to excite a zero-order optically bright state whose wavefunction is spread over many eigenstates.[2,6]

QB spectroscopy can be used to probe the optically dark HVES in the electronic ground state. Coupling of an HVES with an optically bright rovibronic level of an electronically excited state in close proximity would result in a pair of

† Part of the "Sheng Hsien Lin Festschrift".

* Corresponding author. E-mail: hldai@temple.edu.

10.1021/jp075142v CCC: $37.00
Published on Web 09/08/2007

molecular eigenstates each consisting of a part of the optically bright wavefunction for optical excitation.[16,18,25] The HVES level can then be accessed through coherent excitation of the pair of eigenstates. In this approach, the HVES level can be populated and measurements on properties such as collision energy transfer cross section can thus be made for this single HVES.

QBs have been observed in the $\tilde{C}^1B_2 \leftarrow \tilde{X}^1A_1$ bands of SO_2[18]. These QBs arise from vibronic coupling between the low-vibrational levels in the $\tilde{C}^1B_2$ state and the HVES in the $\tilde{X}^1A_1$ state. Xue et al.[16] first demonstrated the use of QB in this region to measure the collision relaxation cross section of a single HVES at 44877.52 cm^{-1} above the zero point at room temperature. Later, this kinetic QB spectroscopy has been applied in the supersonic jet condition[25] so that QB transitions can be isolated from other close-by rovibronic transitions. Collision-induced dephasing cross sections[26] by inert gases and quenching cross section by CO[25] were measured under this condition.

It is rare to find singlet−singlet coupling, such as the one[18] between the $\tilde{C}^1B_2$ and $\tilde{X}^1A_1$ states of SO_2. The matrix element of this vibronic coupling is so small that QB spectroscopy can even be conducted with nanosecond laser pulses. These QBs provide an unusual opportunity to access the single vibrational levels with very high energies, which in this case is just below the dissociation limit at 45 725 cm^{-1} of the $\tilde{X}^1A_1$state, and to characterize their collision relaxation behavior one state at a time. In this paper, we present the many QBs detected in the vibronic bands leading to the (210), (140), and (132) levels of the $\tilde{C}^1B_2$ state of SO_2 under supersonic jet condition. The decay of the fluorescence QB as a function of molecular density in the supersonic jet has been examined for the extraction of collision-induced depopulation cross sections of that specific HVES. All together collision relaxation cross sections of 13 HVES in the electronic ground state with energies ∼45 000 cm^{-1} have been obtained. It is found that there is a correlation between the depopulation cross section and the coupling matrix element between the $\tilde{C}^1B_2$ and $\tilde{X}^1A_1$ states as well as the density of the HVES.

II. Experimental Section

The excitation source is an Excimer laser (Lambda Physik EMG 201) pumped dye laser (Lambda Physik FL3002E). The laser output has a 0.06 cm^{-1} bandwidth full width at half-maximum and 10 ns pulse duration in the laser dye Coumarine 120 region. The output of the dye laser was doubled by a BBO crystal mounted in an autotracking system (Inrad Autotrack II). The doubled laser pulse energy was adjusted to about 50 μJ by using the attenuator in the dye laser to avoid saturating the molecular transitions. The laser beam intersected the supersonic beam of a gas mixture with 1% SO_2 in CO carrier gas (Matheson, UHP grade) 3.88 mm downstream from the nozzle with a 350 μm orifice. The molecular density in the region of the supersonic beam that intersected with the laser was controlled by the stagnation pressure, which was measured by a capacitance manometer (MKS, 0−10 000 Torr).

Laser-induced fluorescence was collected by a PMT (Hamamatsu R2256) through a pair of 2 in. diameter f1 lenses. A masking slit (1 mm width) and a long pass filter (from 220 nm) were used to reduce the Doppler width and scattered light. The fluorescence decay signal was processed by a 400 MHz transient digitizer (Tektronix TDS 380, 2 ns rise time) and averaged 256 times for better S/N ratio. For recording the fluorescence excitation spectrum, a boxcar (Stanford SR250) in conjunction with an A/D board and a personal computer was used for processing the signal.

III. Results and Analysis

In analyzing collision-induced phenomena, it is important that the local pressure and temperature in the laser-jet interaction zone be known. We first describe how these parameters in the supersonic jet are determined.

A. Temperature and Pressure in the Supersonic Jet. There have been extensive theoretical modeling of the molecular density and translational temperature in a supersonic jet following adiabatic expansion through a nozzle.[29,30] The details of the calculation that we use here have been described somewhere else.[25,26] Here, we present a brief description of the calculation.

Because the molecular density drops dramatically in the beam away from the nozzle, to maintain a constant, nonvarying molecular density in this study of collision relaxation the interaction region between the laser and the supersonic jet is chosen to be at the distance of 11D (D is the diameter of the nozzle). At this distance from the nozzle, the density of the beam and translational temperature are calculated to be 2.52×10^{16} molecules/cm^3 and 17 K, respectively, for a stagnation pressure of 1000 Torr. The quality of the calculation is indicated by comparing the calculated translational temperature, 17 K, and the experimentally measured rotational temperature, 18.9 K, at this laser-jet intersection position. The calculated molecular density indicates that in this laser-jet intersection region several collisions would occur for the laser-excited molecules on the time scale of the experiment. Throughout the pressure dependent experiments, the stagnation pressure used was from 300 to 1500 Torr, which resulted in densities ranging from 7.5×10^{15} to 3.8×10^{16} molecules/cm^3 in the intersection region.

B. Fluorescence Excitation Spectrum. The fluorescence excitation spectrum of the $\tilde{C}^1B_2(210) \leftarrow \tilde{X}^1A_1(000)$ band, obtained for the supersonic jet condition described in Subsection A, is shown in Figure 1. Over all the rovibronic transitions for the three bands leading to the (210), (140), and (132) vibrational levels in the $\tilde{C}^1B_2$ state, 30 transitions were found to display QB. Thirteen of these QB transitions are of sufficiently good quality for the single HVES study. These QB transitions are listed in Table 1. Note that the rotational transitions associated with the upper vibrational (132) level, however, cannot be assigned. There are two reasons for this deficiency in spectral assignment.[32] There exists a strong Fermi resonance ($\nu_1 - 2\nu_3$) between the ν_1 (symmetric stretch) and ν_3 (antisymmetric stretch) modes. In addition, there is strong C-axis Coriolis interaction that results in an extraordinarily large C rotational constant and large defect in moment of inertia.[32] These couplings prohibit straightforward and definitive assignment of the rotational transitions. Therefore, we label these transitions only by a series of numbers. These QBs are differentiated from each other by the fitted mixing coefficients and the oscillation frequency, which are listed in Table 1.

C. Kinetic Quantum Beat Spectroscopy. To describe the observed QBs, we first define the two-level system, which is illustrated in Figure 2, and relate them to the SO_2 quantum states. The optically bright level $|B\rangle$ is a rotational level in one of the low-vibrational levels of the $\tilde{C}^1B_2$state. The optically dark level $|D\rangle$ is an HVES of the ground electronic state. The two zero-order levels are separated by ΔE_{bd} and coupled through the matrix element V_{bd}. The two resultant eigenstates, $|1\rangle$ and $|2\rangle$, are linear combinations of the bright and dark levels, $|1\rangle = C_{1b}|B\rangle + C_{1d}|D\rangle$, $|2\rangle = C_{2b}|B\rangle + C_{2d}|D\rangle$, and are separated by

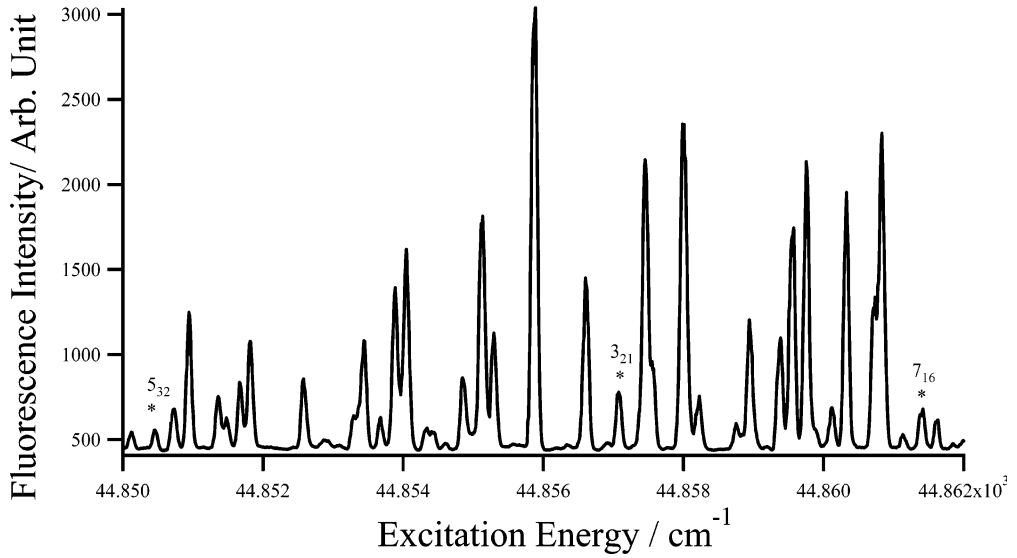

Figure 1. The fluorescence excitation spectrum of the $\tilde{C}^1B_2(210) \leftarrow \tilde{X}^1A_1(000)$ band for SO_2 (1%) in CO in a supersonic expansion. Transitions indicated with * are the ones displaying quantum beat.

TABLE 1: The 13 Fluorescence Quantum Beat Transitions Observed in the Three Vibrational Levels of the $\tilde{C}^1B_2$ State and the Relevant Parameters Deduced from the Two-Level Coupling Model Analysis of the Beat Pattern

vib assignment of the bright level	rot assignment of the bright level	C_{1b}^2/C_{2b}^2 bright level distribution	W_{12}/MHz beat frequency
(210)	3_{21}	0.23:0.77	38.0
	5_{32}	0.14:0.86	16.4
	7_{16}	0.50:0.50	20.9
(140)	7_{25}	0.18:0.82	18.5
	$13_{0,13}$	0.23:0.77	35.9
(132)	1	0.14:0.86	16.9
	2	0.35:0.65	30.9
	3	0.21:0.79	44.1
	4	0.28:0.76	47.9
	5	0.22:0.78	66.1
	6	0.17:0.83	27.8
	7	0.50:0.50	27.7
	8	0.23:0.77	49.7

ΔE_{12}, which is mimicked as the oscillation frequency w_{12} in the QB as $\Delta E_{12} = \hbar w_{12}$.

The time dependence of the fluorescence can be rigorously described as[16,26,31]

$$I(t) \propto C_{1b}^4 \exp(-\gamma_1 t) + C_{2b}^4 \exp(-\gamma_2 t) + 2\xi \mathrm{Re}\{|C_{1b}|^2|C_{2b}|^2 \exp(-((\gamma_1+\gamma_2)/2 + \gamma_{12}^{(de)})t) \times \exp(-i(w_{12}t + \theta))\} \quad (1)$$

where w_{12} is the QB frequency, θ is the initial phase difference between fluorescence from the two eigenstates, γ_1 and γ_2 are the respective depopulation rate constants of the eigenstates, $\gamma_{12}^{(de)}$ is the rate constant for the collision-induced pure dephasing process between the two eigenstates,[26] and ξ is a parameter representing the effect of partial coherence of the optical excitation source.[31] Using this equation to fit the observed QB pattern, we can deduce the mixing coefficients and the coupling matrix element between the bright and dark levels. We note that even with substantial rotational cooling in supersonic jet conditions rotational transitions are still congested in the fluorescence excitation spectrum. Of the many QBs observed, a few of them would have contribution to the fluorescence intensity from other transitions. In this case, a single-exponential decay with a relaxation rate constant (γ_b) and a weighted ratio (B), $B \exp(-\gamma_b t)$, was added to eq 1 to account for the background intensity.[16]

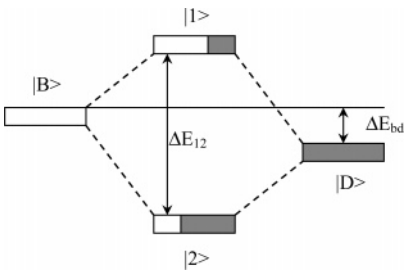

Figure 2. Schematic diagram depicting the eigenlevels and the zero-order bright and dark levels in coupling.

Two typical QB patterns are shown in Figure 3: one is associated with the excitation of a rotational level within the (132) band and the other from the $5_{32}(210)\tilde{C}^1B_2 \leftarrow 4_{22}(000)\tilde{X}^1A_1$transition. The values of the parameters in eq 1 obtained from all the QBs detected are summarized in Table 1.

Both the depopulation and dephasing processes affect the QB decay.[26] The contribution of dephasing is represented by the rate constant $\gamma_{12}^{(de)}$ in eq 1. This parameter describes primarily the decay of the magnitude of the oscillation whereas the depopulation rate constants describe the decay of the overall magnitude. In the analysis of eq 1, pure-dephasing, which is caused by elastic collisions, can be quantitatively separated from depopulation decay. The fitting results show that the pure-dephasing rate in the QBs is negligible in comparison with the depopulation rates, which is consistent with the findings in previous studies.[25,26]

Because the two eigenstates are exclusively derived from the two zero-order bright and dark levels, the sum of the depopulation rate constants of eigenstates should be equal to the sum of those of the zero-order levels, that is, $\gamma_1 + \gamma_2 = \gamma_b + \gamma_d$.[34] Each depopulation rate constant consists of a pressure-dependent and a pressure-independent part. From the fitting of the QB pattern observed at a particular stagnation pressure, $\gamma_1 + \gamma_2$ can be obtained for the calculated corresponding pressure at the interaction zone of the supersonic jet. From a Stern−Volmer plot of $(\gamma_1 + \gamma_2)$ as a function of the calculated molecular density at the interaction region, the pressure-dependent part

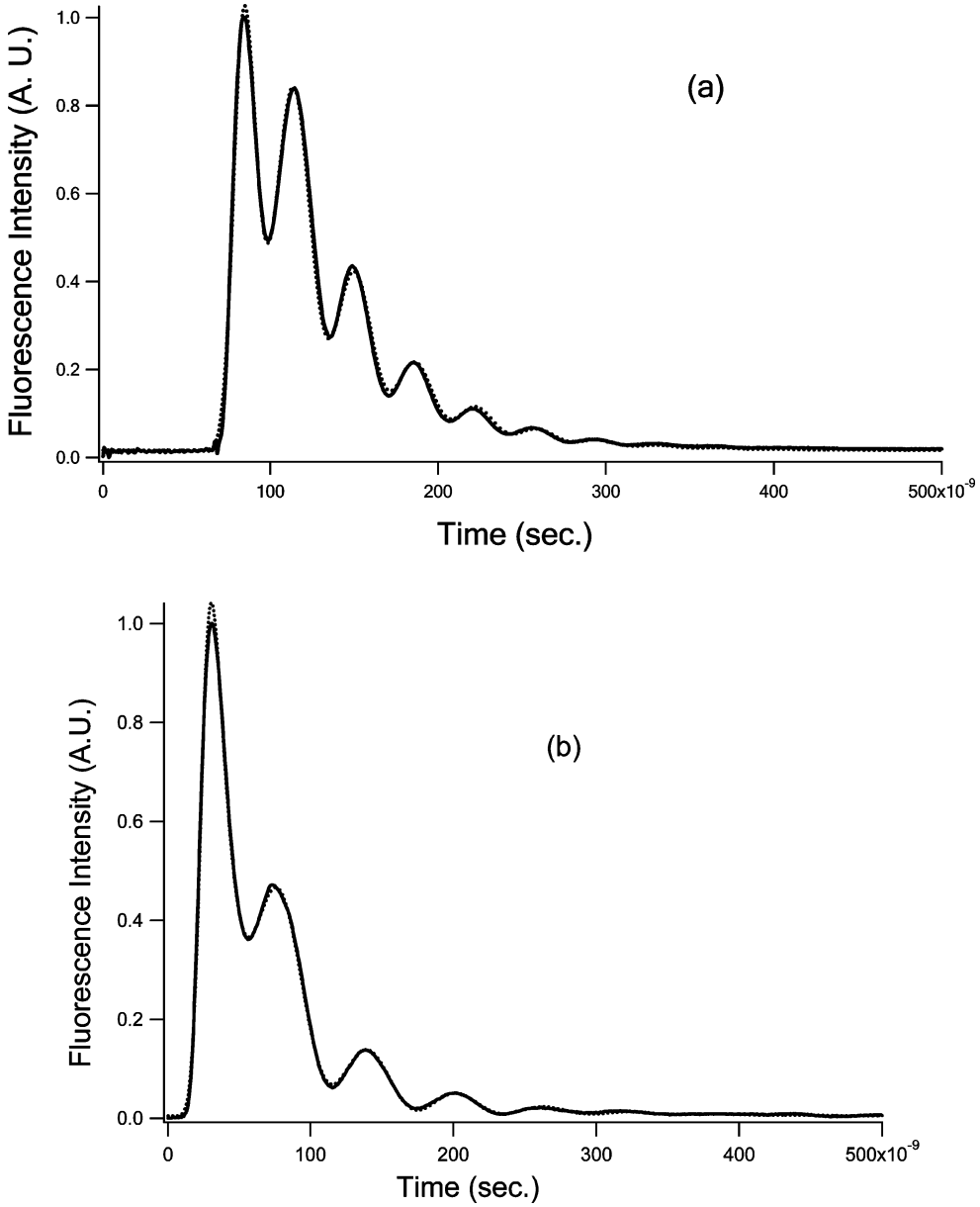

Figure 3. Two fluorescence QB patterns: (a) is from one transition within the (132) band (labeled as number 8 in Tables 1 and 2), and (b) is from one transition in the $5_{32}(210)\tilde{C}^1B_2 \leftarrow 4_{22}(000)\tilde{X}^1A_1$ band. The solid line is the experimental result while the dotted line is the fitting using the two-level coupling model.

of the depopulation rate constant can be extracted from the slope and the pressure-independent part as the intercept.[25]

The depopulation rate constant of the dark, highly vibrationally excited level can be obtained if we know the value of the depopulation rate constant of the bright $\tilde{C}^1B_2$ state level. Although we cannot measure the depopulation constant for the particular bright level involved in the coupling, it is reasonable to assume that its value is similar to that of other nearby rovibronic levels that do not couple to a dark level.[16] This assumption can be examined by measurements of the depopulation rate constants of several bright $(210)\tilde{C}^1B_2$ rotational levels that do not couple to dark levels. These rate constants range from 3.14×10^{-11} to 3.67×10^{-11} cm^3 molecule^{-1} s^{-1}. Thus, an averaged value of 3.44×10^{-11} cm^3 molecules^{-1} s^{-1} is used to represent a generic depopulation rate constant of the bright rotational levels of the $(210)\tilde{C}^1B_2$ state. This process is conducted for each of the vibrational bands of interest in the $\tilde{C}^1B_2$state here.

By subtracting the bright state depopulation rate constant from the sum of the depopulation rate constants of the eigenstates, we obtain the depopulation rate constant for the single, dark HVES in the $\tilde{X}^1A_1$ state. The values for all the single HVES we have examined are listed in Table 2. Using the calculated translational temperature to obtain the collision velocity in the observation region in the supersonic jet, we can deduce the collision-induced depopulation cross sections for these HVES, which are also presented in Table 2.

IV. Discussion

Past experimental and theoretical works on HVESs have been on radiationless processes in which transitions from one bright level to many dark levels occur.[2,35,36] In this study, we examine coupling between a single HVES and a bright level on a one-to-one basis. The measurements of collision-induced depopulation cross section of the single HVES provide a rare opportunity to examine the properties of the single HVES.

The averaged collision-induced depopulation cross section of all 13 levels is 71 Å^2. Compared with the hard sphere cross section, 48 Å^2 for SO_2-CO, the measurements show that even

TABLE 2: Experimentally Measured Depopulation Rate Constants and Cross Sections for the Bright and Dark Levels, Respectively, the Corresponding Vibronic-Coupling Matrix Elements between the Bright and Dark Levels, and Properties of the Dark Levels Such as the Total Energy, the Rovibronic Symmetry, and the Total Angular Momentum

rot assign	$\bar{\gamma}_b^{pb}$	γ_d^{pa}	$\bar{\sigma}_b$/Å^{2a}	σ_d/Å^{2a}	V_{bd}/MHz^a	energy cm^{-1}	rovibronic symmetry	total AM
3_{21}	3.4 (0.2)	7.4(2.0)	25.3 (1.5)	55(15)	14.4(1.0)	44865.8	A_1	3
5_{32}		3.7(1.0)		27(8)	8.9(0.7)	44875.4	A_2	5
7_{16}		6.3(1.6)		47(12)	10.5(1.3)	44877.0	A_2	7
7_{25}	7.0 (0.8)	5.1(1.6)	52 (0.6)	38(12)	8.0(0.7)	45043.7	A_1	7
$13_{0,13}$		6.8(3.2)		50(24)	17.6(0.8)	45079.6	A_1	13
1	7.2 (0.6)	8.0(0.2)	53 (0.4)	59(8)	9.4(1.0)	45340.9	A	N/A
2		25.4(3.9)		187(29)	15.7(0.7)	45344.3	A	N/A
3		4.8(2.0)		35(15)	15.4(0.5)	45342.5	A	N/A
4		7.8(2.4)		57(18)	29.9(0.1)	45343.0	A	N/A
5		9.0(0.76)		66(6)	24.9(0.2)	45341.8	A	N/A
6		6.8(1.8)		50(13)	11.3(1.3)	45329.6	A	N/A
7		25.4(4.0)		187(29)	13.9(0.1)	45341.4	A	N/A
8		8.5(0.9)		63(7)	21.4(0.8)	45343.0	A	N/A

[a] The value inside the bracket is one standard deviation of the fitting results. [b] In unit of 10^{-11} cm^3 molecule^{-1} s^{-1}.

under the condition of low-collision energy in the supersonic beam, the collision cross section is larger than the hard sphere. Because repulsive force-related collision quenching is relatively inefficient at low temperature, such as described by the SSH (Schwartz−Slawsky−Herzfeld) theory,[37,38] this large cross section can not be solely accounted for by the short-range repulsive force. There has to be a significant contribution from interactions, such as the ones mediated through transition dipoles,[12] in addition to the repulsive force in collision energy transfer from highly vibrationally excited SO_2 to the collision partner CO.

In the following, we examine the relation between the depopulation cross sections with the rovibronic symmetry, the total angular momentum, and the total energy of the HVESs and the vibronic-coupling matrix elements between the HVESs and their corresponding bright levels.

A. Depopulation Cross Section of the HVESs and Their Rovibronic Symmetry and Total Angular Momentum. Collision-induced population relaxation from the HVES may relate to the symmetry and the total angular momentum of the HVES because these parameters determine the density of the levels for the depopulation channels and the magnitude of the coupling matrix elements. Though the complete set of rotational and vibrational quantum numbers for the HVES with more than 44 500 cm^{-1} rovibrational energy are not assignable, the rovibronic symmetry and total angular momentum remain good quantum numbers that can be deduced from the optically bright level in coupling with the HVES.[39−41]

The nonzero vibronic-coupling matrix element, $\langle \Psi_{ev}^{B}|H'|\Psi_{ev}^{D}\rangle$, requires that the direct product of symmetry species, $\Gamma(\Psi_{ev}^{B}) \otimes \Gamma(H') \otimes \Gamma(\Psi_{ev}^{D})$, contain the A_1 representation in the C_{2v} point group.[40] Because in the energy region of concern it is anticipated that Coriolis interaction mixes the vibrational and rotational wavefunctions, $\Gamma(\Psi_{evr})$ instead of $\Gamma(\Psi_{ev})$ should be used in the discussion of the symmetries of the bright and dark levels. The vibronic symmetry of $\tilde{C}^1B_2(210)$, (140), and (132) is B_2.[32] The rotational wavefunction of the bright level has either B_1 or B_2 symmetry depending on the rotational quantum numbers. Because H' has A_1 symmetry and the same for the ground electronic state, the rovibrational symmetry for the HVESs should be either A_1 or A_2. Because of the lack of rotational assignment for the levels in the $(132)\tilde{C}^1B_2$ vibronic level,[32] we can only designate the rotational symmetry as $\Gamma(\Psi_r^b) = B$ with respect to the C_2 axis in C_{2v} group. The corresponding HVES monitored in this band can only be labeled with A representation.

Both bright and dark rovibronic levels in coupling should have the same total angular momentum. Because of Coriolis interaction, K is no longer a good quantum number for the rotational levels in this energy region.[39] Again, because there is no rotational assignment for the bright rotational levels in the $(132)\tilde{C}^1B_2$ vibronic level, no information on the total angular momentum is available for their corresponding dark HEVS levels. The total angular momenta of the other five HVESs coupled with rotational levels within the (210) and (140) vibronic levels can be obtained through the rotational assignment of their coupled bright levels. The total symmetry and angular momentum of the HEVSs are listed in Table 2.

The experimentally measured collision-induced depopulation cross sections do not show obvious dependence on either the symmetry of the HVESs or their total angular momentum within this limited set of data. The fluctuations in cross section, like other molecular properties, perhaps reflect the stochastic nature of the vibrational levels in high-energy regions.

B. Depopulation Cross Section of the HVESs and the Total Internal Energy. The energy of a HVES can be determined from the energy of the bright level in coupling with the HVES, because the energy difference between the bright level and the HVES level is comparable within the quantum beat frequency of 10∼30 MHz. Because there is no rotational assignment made for the levels in $(132)\tilde{C}^1B_2$, the energy of the bright levels in this vibrational band cannot be determined precisely. The energies of the HVESs coupled with the bright levels in this band therefore are simply represented by the laser photon excitation energies, considering that the magnitude of the total energy is much larger than the small uncertainty associated with the rotational energy of the bright levels. The depopulation cross sections measured for the HVESs are plotted against their total energies in Figure 4. It appears that the depopulation cross sections increase slightly with the total energies of the HVESs.

The vibrational level densities in the regions of 44 871, 45 061, and 45 341 cm^{-1} above the zero-point energy are calculated to be 3.02, 3.05, and 3.09, respectively.[32] The density increases slightly over this small increase of energy. This small increment in density appears to be correlated with an increase with large fluctuation in the depopulation cross sections of HVES (Figure 4). This correlation can be understood through several possibilities. Higher density simply means that more collision energy transfer channels are available at the same energy. Also, with increased level density, the energy difference

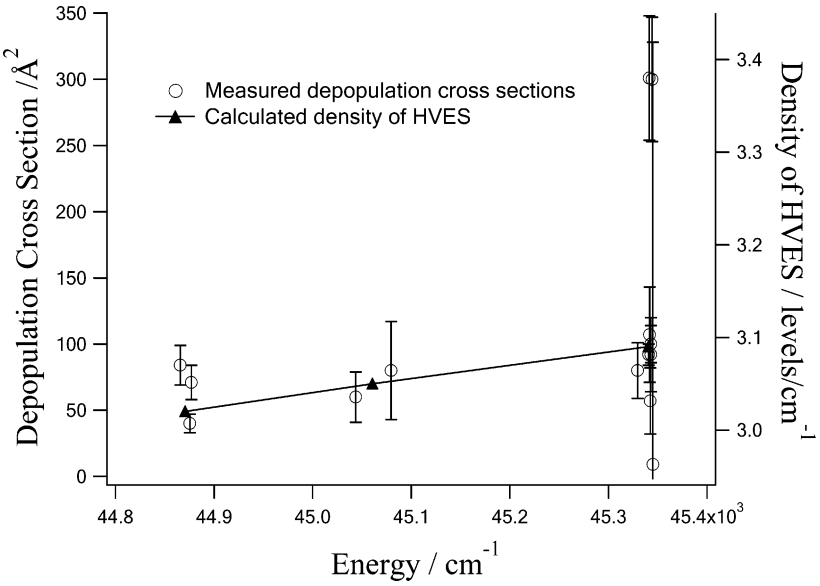

Figure 4. Depopulation cross sections and HVES level densities plotted as a function of the total energy.

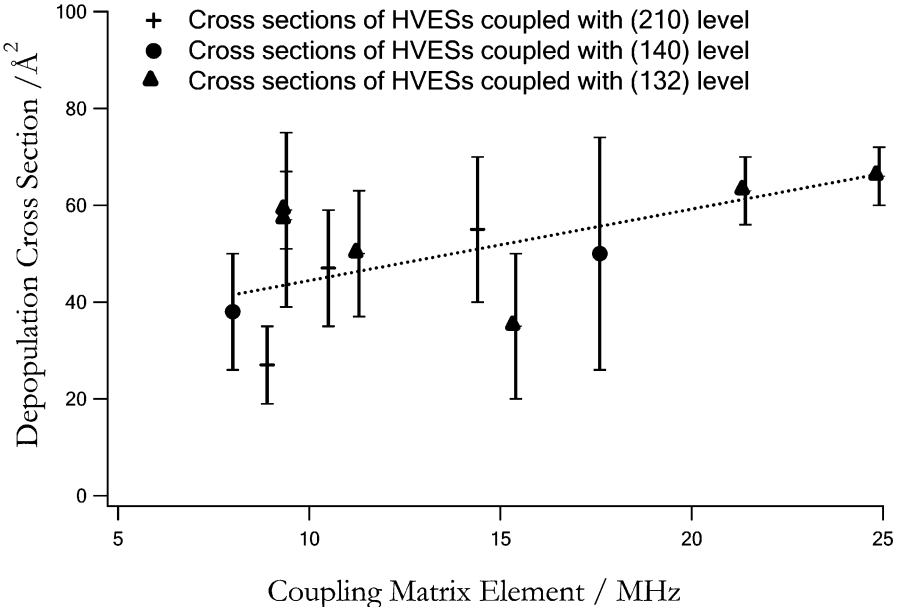

Figure 5. Depopulation cross sections of the HVESs are plotted as a function of the corresponding coupling matrix elements. A linear trend represented by the dotted line is shown as aid to the eye.

between the HVESs becomes smaller, which facilitates more efficient $V-T$ energy transfer.

C. Correlation between Depopulation Cross Sections and Coupling Matrix Elements between the "Bright" and "Dark" Levels. The vibronic-coupling matrix elements between the dark and bright levels can be obtained from the analysis of the observed quantum beat pattern.[34] The measured coupling matrix elements are presented in Table 2. These coupling matrix elements are plotted against the corresponding depopulation cross sections of the HVESs in Figure 5. This plot allows us to examine whether there is a correlation between the two quantities and infer if there is a common property of the HVESs that is responsible for both collisional relaxation and intramolecular vibronic coupling. Indeed, Figure 5 shows that in general the HVES that has the stronger vibronic-coupling matrix element does have a larger collisional relaxation cross section.

To understand this correlation, we first examine the origin of the matrix element between the coupled bright and dark levels. The vibronic-coupling matrix element, V_{bd}, resulting from the breakdown of the Born−Oppenheimer approximation, can be written as[41]

$$V_{bd} = \langle \Phi_b(q,Q)\Lambda_b(Q)|T^N(Q)|\Phi_d(q,Q)\Lambda_d(Q)\rangle \qquad (2)$$

Here, q and Q are the coordinates for the electrons and nuclei, respectively, $\Phi(q,Q)$ is the electronic wavefunction, and $\Lambda(Q)$ is the vibrational wavefunction. The subscripts b and d refer to the bright and dark levels, respectively. The nuclear kinetic energy operator that is omitted in the Born−Oppenheimer approximation because of the large mass value of the nuclei in the denominator is

$$T^N(Q) = -\sum_i \left(\frac{\hbar^2}{2\mu_i}\right)\frac{\partial^2}{\partial Q_i^2} \qquad (3)$$

By taking the largest contribution from the first-order derivative term of eq 2 and assuming that the magnitude of the vibronic

coupling arises primarily from one specific vibrational mode Q_k, this formula can then be further simplified as

$$V_{bd} \approx -\sum_k \left(\frac{\hbar^2}{\mu_k}\right)\left\langle \Phi_b(q,Q)\left|\frac{\partial}{\partial Q_k}\right|\Phi_d(q,Q)\right\rangle \int_Q \Lambda_b(Q)\,\frac{\partial}{\partial Q_k}\Lambda_d(Q)\,dQ$$
$$\approx -(\hbar^2\mu_k\left\langle \Phi_b(q,Q)\left|\frac{\partial}{\partial Q_k}\right|\Phi_d(q,Q)\right\rangle \times \left\langle \Lambda_b(Q_k)\left|\frac{\partial}{\partial Q_k}\right|\Lambda_d(Q_k)\right\rangle \underline{\prod_{i\neq k}\langle\Lambda_b(Q_i)|\Lambda_d(Q_i)\rangle} \quad (4)$$

where $|\Lambda(Q)\rangle = |\Lambda(Q_k)\rangle \prod_{i\neq k}|\Lambda(Q_i)\rangle$. The last term underlined in eq 4 is a Franck−Condon overlap for all the vibrational modes other than the coupling vibrational mode, Q_k.

Now, we consider how to relate the depopulation cross section of the HVES to its wavefunction. The population of a specific HVES level could relax to other HVESs or bright levels after a collision. If the relaxation process is induced through electromagnetic interaction, $V(t)$, between the collisional partners, the transition possibility from the HVES to other levels can be expressed, according to the time-dependent perturbation theory, as

$$P_{if}(t) = \frac{1}{\hbar^2}\left|\int_0^t e^{iw_{if}t'}\langle\Psi_i|V(t')|\Psi_f\rangle\,dt'\right|^2 \quad (5)$$

It is reasonable to assume that the transition dipole moment is independent of time and can be extracted from the integral

$$P_{ij}(t) \propto |\langle\Psi_i|\mu|\Psi_j\rangle|^2 f(t) \quad (6)$$

Considering that there are two types of final levels after collision relaxation, the HVES and the bright level, we express the total depopulation cross section σ of the initial HVES with contributions from the two competing channels

$$\sigma \propto C_{bright}(t,b,T)^*|\langle\Psi_d^i|\mu|\Psi_b^f\rangle|^2 + C_{dark}(t,b,T)^*|\langle\Psi_d^i|\mu|\Psi_d^f\rangle|^2$$
$$\propto C_{bright}(t,b,T)^*|\underline{\Lambda_d^i(Q)|\Lambda_b^f(Q)}|^2|\langle\tilde{X}|\mu_e|\tilde{C}\rangle|^2 + C_{dark}(t,b,T)^*|\langle\Lambda_d^i(Q)|\mu_N|\Lambda_d^f(Q)\rangle|^2 \quad (7)$$

$C(t,b,T)$ is a parameter that depends on the integral of time, collision impact parameter b, and the Boltzmann distribution at temperature T. The transition dipole operator relation, $\mu = \mu_e + \mu_N$, is used.[12] $|\tilde{X}\rangle$ and $|\tilde{C}\rangle$ are the electronic wavefunctions for the dark and bright levels, respectively.

The depopulation cross section is found to depend on the square of the Franck−Condon factor, $|\langle\Lambda_d^i(Q)|\Lambda_b^f(Q)\rangle|^2$, which is underlined in eq 7. The appearance of the Franck−Condon overlap between the bright and dark levels in both expressions for the vibronic-coupling matrix element and the collision-induced depopulation cross section suggests the origin of their correlation. In Figure 5, it is not straightforward to differentiate whether the correlation between the depopulation cross section and the vibronic-coupling matrix element is linear or quadratic although a quadratic relation is predicted in the equations.

A similar correlation between the deactivation cross section and the Franck−Condon overlap was observed in collision-induced deactivation of CN.[42] A semiempirical model was proposed for describing the measured deactivation cross section of CN as proportional to the energy gap, ΔE, between the initial and final vibrational levels in different electronic states and the Franck−Condon overlap between these two vibrational levels, $\langle\Lambda_b(Q)|\Lambda_d(Q)\rangle$:

$$\sigma \propto \langle\Lambda_b|\Lambda_d\rangle \exp\left(-\frac{\Delta E}{kT}\right) \quad (8)$$

With a sufficiently small energy difference between the coupled bright and dark levels in comparison with kT, the depopulation cross section should be linearly dependent on the Franck−Condon overlap.

This connection between the vibronic-coupling matrix element and the depopulation cross section through the Franck−Condon overlap highlights the importance of similar vibrational wavefunctions of the initial and final levels in the collision energy transfer process when the two levels are in two different electronic states. Because the nature of the interaction is also electromagnetic, this dependence is similar to that of the optical transition between electronic states. This particular correlation that has been identified supports the notion that relaxation of highly vibrationally excited levels involves substantial contributions from long range interactions.[25,35]

D. Temperature Dependence in Depopulation Cross Sections. The collision-induced depopulation cross section measured in supersonic jet conditions is much different from the one acquired in a static cell at room temperature. Previously, the depopulation cross section at room temperature of the HVES coupled with the $7_{16}(210)$ $\tilde{C}^1B_2$ rovibronic bright level was measured[16] as 231 Å^2. In this work performed in the supersonic jet, a much smaller value of 71 Å^2 as an average of the 13 measured cross sections is measured for the translational temperature of about 17 K.

The temperature effect for short versus long range interactions, which may both contribute to collision energy transfer of highly vibrationally excited molecules, should be very different. The smaller relative velocity between the excited molecule and the collisional partner at low-translational temperature will increase the interaction time in a collision. It increases the energy transfer efficiency through the long range interaction. The cross section should subsequently increase, rather than decrease, at a lower temperature. Therefore, the observed decrease of the cross section must arise from the contribution from the short-range repulsive force. Such decrease related to repulsive force-induced energy transfer is understandable because the large amount of momentum transfer associated with energy transfer in a repulsive collision is difficult to achieve at a much reduced velocity. According to the SSH theory, a decrease of temperature from 298 to 17 K corresponds to a reduction by more than 2 orders of magnitude in collision energy transfer efficiency.[7,8] Thus, it is reasonable to speculate that the measured depopulation cross sections in supersonic jet conditions are primarily from the long range interaction contribution.

This comparison signifies that substantial portions of the relaxation cross section of highly vibrationally excited molecules arise from both the repulsive force and the long range interaction. However, the relative significance of the two contributions differs according to the temperature.

V. Conclusion

Collision-induced depopulation cross section of 13 single, highly vibrationally excited levels with ~45 000 cm^{-1} energy in the electronic ground state of SO_2 by CO has been measured. The collision relaxation properties of these single HVESs are examined through pressure dependence of the decay of the fluorescence quantum beat resulted from their coupling with

the optically bright rovibronic levels in the (140), (210), and (132)$\tilde{C}^1B_2$bands.

The depopulation cross section measured for the 13 highly vibrationally excited levels range from 27 to 187 Å^2. The averaged depopulation cross section at the low temperature of 17 K of all 13 HVES, ~71 Å^2, is much larger than the hard sphere cross section of 48 Å^2 and indicates efficient energy transfer for a HVES through long range interactions. It is found that the depopulation cross section does not depend on the symmetry and the angular momentum of the HVES, though it increases slightly with the total energy of the HVES. This increase is likely due to the increasing level density of the HVESs with energy. In addition, a trend in that the depopulation cross section of the HVESs increases with the vibronic-coupling matrix element between the HVES and the corresponding bright level is identified. This correlation can be understood from the Franck−Condon factor depicting the overlap between the vibrational wavefunctions of the two coupled levels. This factor appears in both the coupling matrix element as well as the depopulation probability through electromagnetic interactions. The comparison of the depopulation cross section in the supersonic jet as well as the room temperature measurements show that relaxation of the HVESs at low temperature is primarily through the long range interaction and that both long and short range interactions contribute significantly at higher temperatures.

Acknowledgment. This work is supported in part by a grant from the NSF Grant CHE-0111520.

References and Notes

(1) Flynn, G. W.; Parmenter, C. S.; Wodtke, A. M. *J. Phys. Chem.* **1996**, *100*, 12817.
(2) Kommandeur, J.; Majewski, W.; Meerts, W. L.; Pratt, D. W. *Annu. Rev. Phys. Chem.*, **1987**, *38*, 433.
(3) Crim, F. F. *J. Phys. Chem.* **1996**, *100*, 12725.
(4) Zare, R. N. *Science* **1998**, *279*, 1875.
(5) Anderson, S. L. *Acc. Chem. Res.* **1997**, *20*, 28.
(6) Nesbitt, D. J.; Field, R. W. *J. Phys. Chem.* **1996**, *100*, 12735.
(7) Yardley, J. M. *Introduction to Molecular Energy Transfer*; Academy Press: New York, 1980.
(8) Lambert, J. D. *Vibrational and Rotational Relaxation in Gases*; Clarendon: Oxford, 1977.
(9) Flynn, G. W. *Acc. Chem. Res.*, **1981**, *14*, 334.
(10) Weston, R. E.; Flynn, G. W. *Annu. Rev. Phys. Chem.*, **1992**, *43*, 559.
(11) Hartland, G. V.; Xie, W.; Dai, H.-L.; Simon, A.; Anderson, M. J. *Rev. Sci. Instrum.* **1992**, *63*, 3261.
(12) Hartland, G. V.; Qin, D.; Dai, H.-L.; Chen, C. *J. Chem. Phys.* **1997**, *107*, 12890.
(13) Michaels, C. A.; Flynn, G. W. *J. Chem. Phys.* **1997**, *106*, 3554.
(14) Hamilton, C. E.; Kinsey, J. L.; Field, R. W. *Annu. Rev. Phys. Chem.* **1986**, *37*, 493
(15) Special issue on "overtone spectroscopy and dynamics". *Chem. Phys.* **1995**, 190.
(16) Xue, B.; Han, J.; Dai, H.-L. *Phys. Rev. Lett.* **2000**, *84*, 2606.
(17) Demtroder, W. *Laser Spectroscopy*; Springer: New York, 1996.
(18) Ivanco, M.; Hager, J.; Sharfin, W.; Wallace, S. C. *J. Chem. Phys.* **1983**, *78*, 6531.
(19) Vaccaro, P. H.; Zabuludoff, A.; Carren-Patino, M. E.; Kinsey, J. L.; Field, R. W. *J. Chem. Phys.* **1989**, *90*, 4150.
(20) Dupré, P.; Green, P. G.; Field, R. W. *Chem. Phys.* **1995**, *196*, 211.
(21) Knee, J. L.; Doany, F. E.; Zewail, A. H. *J. Chem. Phys.* **1985**, *82*, 1042.
(22) Henke, W.; Selzle, H. L.; Hayes, T. R.; Lin, S. H.; Schlag, E. W. *Chem. Phys. Lett.* **1981**, *77*, 448.
(23) Chang, C. H.; Huang, C.; Ni, C.; Dai, H.-L.; Hayashi, M.; Liang, K. K.; Kuang, A.; Chen, I. C.; Lin, S. H. *Mol. Phys.* **2002**, *100*, 1117.
(24) Kohguchi, H.; Ohshima, Y.; Endo, Y. *Chem. Phys. Lett.* **1996**, *254*, 379.
(25) Zhang, M.; Ma, J.; Han, J.; Dai, H.-L. *J. Chin. Chem. Soc.* **2006**, *53*, 25.
(26) Zhang, M.; Han, J.; Liu, P.; Muller, D.; Dai, H.-L. *J. Phys. Chem. A* **2003**, *107*, 10845.
(27) Brucat, P. J.; Zare, R. N. *J. Chem. Phys.* **1984**, *81*, 2562.
(28) Dupre, P.; Jost, R.; Lombardi, M.; Green, P. G.; Abramson, E.; Field, R. W. *Chem. Phys.* **1991**, *152*, 293.
(29) Anderson, J. B. Molecular Beam from Nozzle Source. In *Molecular Beams and Low-density Gas Dynamics*; Wegener, P. P., Ed.; Marcel Dekker Inc.: New York, 1974; p 1.
(30) Miller, D. R. Free Jet Source. In *Atomic and Molecular Beam Methods*; Scoles, G., Ed.; Oxford University Press: New York, 1988; Vol. 1.
(31) Jiang, X. P.; Brumer, P. *Chem. Phys. Lett.* **1991**, *180*, 222.
(32) Yamanouchi, K.; Okunishi, M.; Endo, Y.; Tsuchiya, S. *J. Mol. Struct.* **1995**, 352/353, 541.
(33) Troe, J. *J. Chem. Phys.*, **1977**, *66*, 4758.
(34) Waite, B. A.; Gray, S. K.; Miller, W. H. *J. Chem. Phys.* **1983**, *78*, 259.
(35) Michaels, C. A.; Mullin, A. S.; Flynn, G. W. *J. Chem. Phys.* **1995**, *102*, 6682.
(36) *Radiationless Transition*; Lin, S. H., Ed.; Academic Press: New York, 1980.
(37) Schwartz, R. N.; Slawsky, Z. I.; Herzfeld, K. F. *J. Chem. Phys.* **1952**, *20*, 1591.
(38) (a) Zhang, M. Ph.D. Thesis, University of Pennsylvania, 2007. (b) Zhang, M.; Dai, H. L. Unpublished work.
(39) Dai, H.-L.; Kopra, C. L.; Kinsey, J. L.; Field, R. W. *J. Chem. Phys.*, **1985**, *82*, 1688.
(40) Herzberg, G. *Molecular Spectra and Molecular Structure*; Van Nostrand Company: New York, 1966; Vol. III, D.
(41) Lefebvre-Brion, H.; Field, R. W. *Perturbations in the Spectra of Diatomic Molecules*; Academic Press: New York, 1986.
(42) Katayama, D. H.; Miller, T. A.; Bondybey, V. E. *J. Chem. Phys.* **1979**, *71*, 1662.